

Wave propagation in a 3D fully nonlinear NWT based on MTF coupled with DZ method for the downstream boundary

G. Xu^{*1,3}, A.M.S. Hamouda¹ and B.C. Khoo²

¹Department of Mechanical and Industrial Engineering, Qatar University, Doha-2713, Qatar

²Department of Mechanical Engineering, National University of Singapore, 10 Kent Ridge Crescent, 119260, Singapore

³School of Naval Architecture and Ocean Engineering, Jiangsu University of Science and Technology, Zhenjiang, China

(Received November 29, 2013, Revised March 26, 2014, Accepted April 4, 2014)

Abstract. Wave propagation in a three-dimensional (3D) fully nonlinear numerical wave tank (NWT) is studied based on velocity potential theory. The governing Laplace equation with fully nonlinear boundary conditions on the moving free surface is solved using the indirect desingularized boundary integral equation method (DBIEM). The fourth-order predictor-corrector Adams-Bashforth-Moulton scheme (ABM4) and mixed Eulerian-Lagrangian (MEL) method are used for the time-stepping integration of the free surface boundary conditions. A smoothing algorithm, B-spline, is applied to eliminate the possible saw-tooth instabilities. The artificial wave speed employed in MTF (multi-transmitting formula) approach is investigated for fully nonlinear wave problem. The numerical results from incorporating the damping zone (DZ), MTF and MTF coupled DZ (MTF+DZ) methods as radiation condition are compared with analytical solution. An effective MTF+DZ method is finally adopted to simulate the 3D linear wave, second-order wave and irregular wave propagation. It is shown that the MTF+DZ method can be used for simulating fully nonlinear wave propagation very efficiently.

Keywords: NWT; DBIEM; multi-transmitting formula; damping zone; MTF+DZ

1. Introduction

When simulating the nonlinear wave propagation through an unbounded domain in the time domain, it is necessary to truncate the computational domain into a finite domain in order to reduce computational cost. Thus, non-reflecting radiation condition is required for the truncated surface, however, there is no exact non-reflecting condition in existence. The Sommerfeld-Orlanski's condition (Orlanski 1976) has been widely used for linear simulation; this condition is local in both time and space and dependent on the phase velocity of out-going wave but cannot ensure good results for irregular wave problem. The global matching or shell function method (Dai and Duan 2008, Newman 2010) can be very accurate for linear irregular wave radiation but with relatively large computational effort on comparing with the local method and still can not fully satisfy the nonlinear condition. Another common used method is Damping Zone

*Corresponding author, Dr., E-mail: xugang131@gmail.com

(DZ) (Baker *et al.* 1981, Sclavounos and Nakos 1989, Cointe *et al.* 1990, Beck *et al.* 1993, Celebi *et al.* 1998, Clamond *et al.* 2005), which can absorb high frequency waves efficiently. However, it is limited by the length of DZ and therefore not very efficient for low frequency waves. Clément (1996) proposed a coupled method (piston-beach hybrid absorber) to absorb outgoing wave. Boo (2002) proposed a numerical scheme, which combines an absorbing beach and the stretching technique (Forristall 1985), to simulate the open boundary. Wang and Wu (2007) imposed a radiation condition via a combination of DZ and Sommerfeld-Orlanski equation. However, the efficiency of DZ method strongly depends on the ratio of the length of damping zone and wave length. The longer wave length requires a wider beach. It will thus result in much more meshes on the free surface, especially when dealing with irregular wave problem.

In order to find a more efficient and feasible radiation condition to deal with fully nonlinear irregular wave problem, a Multi-Transmitting Formula (MTF) method (Liao 1996, 2002) for transmitting waves out of truncated surface, applied as radiation condition, is introduced. In this method, an artificial wave speed is used to replace the physical wave speed. Usually, it is not necessary to make the artificial wave speed equal to physical wave speed. As a result, it is very useful for dealing with irregular wave problem. Recently, the MTF method has been successfully used for simulating harmonic radiation (Xu and Duan 2008a), linear irregular wave diffraction (Xu and Duan 2008b, Zhang and Duan 2012) and two-dimensional fully nonlinear numerical wave tank (NWT) (Duan and Zhang 2009).

In this work, the indirect desingularized boundary integral equation method (DBIEM), which has been successfully used previously in solving nonlinear water wave problems such as in the work by Zhang *et al.* (2006, 2007), is employed to solve the boundary value problem at each time step. Compared with the conventional boundary element method (BEM), the integral kernels of the DBIEM are no longer singular as the singularities are placed slightly outside the fluid domain. This is particularly advantageous when the direct differentiation is applied to the integral equation to obtain the velocity. The fourth-order predictor-corrector Adams-Bashforth-Moulton (ABM4) scheme and mixed Eulerian-Lagrangian (MEL) method are used for the time-stepping integration of the free surface boundary conditions. Since wave breaking is not considered, the position of the nodes on free surface is tracked by applying the semi-Lagrangian approach (Koo and Kim 2007), in which the nodes on free surface are allowed to move only in vertical direction, with the horizontal motion of the nodes on the free surface held fixed. This approach has the advantage of avoiding the task of re-gridding the free surface at each time step. For stable time-step simulation, a B-spline smoothing scheme is applied in both longitudinal and transverse directions of the tank to prevent saw-tooth instability. For the simulation, the DZ, MTF and MTF coupled DZ (MTF+DZ) methods are employed as radiation condition to minimize wave reflection on the truncated surface. As will be shown below, numerical results obtained by the coupled MTF+DZ method agree very well with the analytical solution and show that the present model is effective in the simulation for 3D wave propagation.

2. Mathematical model

A Cartesian coordinate system $oxyz$ is defined for 3D wave propagation problem, as shown in Fig. 1. The origin of $oxyz$ is placed on the plane of the undisturbed free surface with the x -axis positive in the propagation direction of incident wave prescribed at the vertical upstream boundary, and the z -axis positive in the opposite direction of gravity. In Fig. 1, D denotes the fluid domain

while Γ_F , Γ_W , Γ_B , Γ_U and Γ_D denote the boundaries of instantaneous free surface, side wall, bottom, upstream and downstream, respectively.

We assume the fluid is incompressible and inviscid, and the flow irrotational, the fluid motion can be described by a velocity potential ϕ , which satisfies the Laplace equation within the fluid domain D

$$\nabla^2 \phi(x, y, z, t) = 0 \tag{1}$$

All the boundary conditions can be described as follows:

1. On the instantaneous free surface Γ_F , the dynamic and kinematic conditions can be written as

$$\frac{\partial \phi}{\partial t} + \frac{1}{2} \nabla \phi \nabla \phi + g\eta = 0 \tag{2}$$

$$\frac{\partial \eta}{\partial t} + \frac{\partial \phi}{\partial x} \frac{\partial \eta}{\partial x} + \frac{\partial \phi}{\partial y} \frac{\partial \eta}{\partial y} - \frac{\partial \phi}{\partial z} = 0. \tag{3}$$

2. On side wall Γ_W and bottom Γ_B , the zero-normal flux condition can be expressed as

$$\frac{\partial \phi(x, y, z, t)}{\partial n} = 0 \tag{4}$$

3. On upstream boundary Γ_U , the fluid motion is prescribed by giving the properties (surface elevation and normal velocity) of known incident wave.

4. For downstream boundary condition, the fluid domain has to be truncated at a finite downstream boundary Γ_D of the NWT. An appropriate radiation condition should be imposed to minimize the wave reflection during the simulation in time domain.

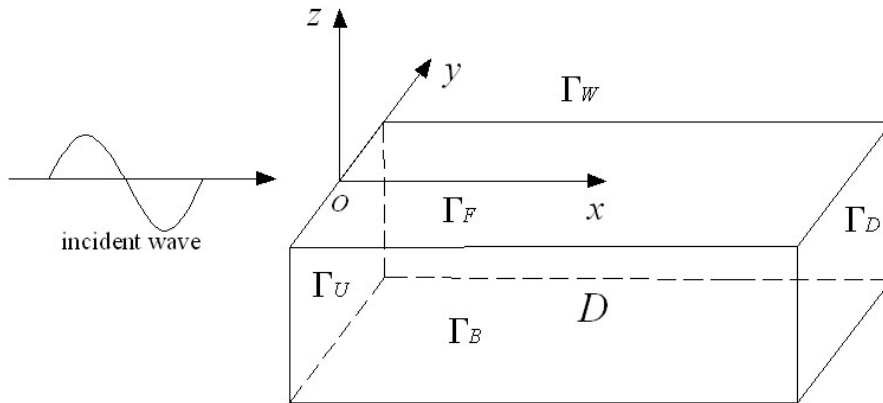


Fig. 1 Sketch of a 3D numerical wave tank

3. Desingularized boundary integral equation method

In this study, the indirect DBIEM is employed to solve the boundary value problem for the unknown velocity potential $\phi(x, y, z, t)$ at each time step. This method obtains the solution by distributing Rankine sources over a surface S outside the fluid domain D . This surface is at a small distance away from the corresponding real boundary of the fluid. The velocity potential in the fluid domain D can be written as follows

$$\phi(p, t) = \iint_S \sigma(q, t) \frac{1}{r_{pq}} ds_q \quad (5)$$

where $q(\xi, \eta, \zeta)$ is the integration point on the integration surface S outside the fluid domain, $p(x, y, z)$ is the field point where the potential is evaluated, σ is the unknown source strength distribution over the surface S and

$$r_{pq} = \sqrt{(x - \xi)^2 + (y - \eta)^2 + (z - \zeta)^2} \quad (6)$$

For the problem considered in this work, we construct the solution using a constant-strength source point within each element over the integration boundary S_F and a constant-strength source point over the integration surface S_W , where S_F is the integration surface above the free surface Γ_F , and S_W is the integration surface outside the real boundary of the tank. That is

$$\phi(p, t) = \iint_{S_F} \sigma_F(q, t) \frac{1}{r_{pq}} ds_q + \iint_{S_W} \sigma_W(q, t) \frac{1}{r_{pq}} ds_q \quad (7)$$

By applying the boundary conditions, we obtain boundary integral equations for the unknown strength of the singularities, $\sigma_F(q, t)$ and $\sigma_W(q, t)$, respectively

$$\iint_{S_F} \sigma_F(q, t) \frac{1}{r_{pq}} ds_q + \iint_{S_W} \sigma_W(q, t) \frac{1}{r_{pq}} ds_q = \phi_0(p, t) \quad (8)$$

$$\iint_{S_F} \sigma_F(q, t) \frac{\partial}{\partial n_p} \left(\frac{1}{r_{pq}} \right) ds_q + \iint_{S_W} \sigma_W(q, t) \frac{\partial}{\partial n_p} \left(\frac{1}{r_{pq}} \right) ds_q = \frac{\partial \phi_0(p, t)}{\partial n_p} \quad (9)$$

In the desingularized method, the source distribution is outside the fluid domain so that the source points never coincide with the field points and therefore the integrals are non-singular. In addition, because of the desingularization, we can use simple isolated Rankine sources and obtain the equivalent accuracy. This greatly reduces the complexity of the form of the influence coefficients that make up the elements of the kernel matrix (Zhang *et al.* 2006). Then the integral equations in Eqs. (8) and (9) can be replaced by a discrete summation of N -isolated singularities located at a small distance away from the corresponding control point on the boundaries

$$\sum_{i=1}^N \sigma(q_i, t) \frac{1}{r_{pq_i}} = \phi_0(p, t) \quad (10)$$

$$\sum_{i=1}^N \sigma(q_i, t) \frac{\partial}{\partial n_p} \left(\frac{1}{r_{pq_i}} \right) = \frac{\partial \phi_0(p, t)}{\partial n_p} \quad (11)$$

The desingularized distance between isolated source point and corresponding control point is given by

$$L_d = l_d (D_m)^\beta \quad (12)$$

where l_d and β are constants and D_m is a measure of the local mesh size (typically the square root of the local mesh area). The accuracy and convergence of the solutions are sensitive to the choices of l_d and β . Therefore, appropriate l_d and β values need to be determined after numerical test. The recommended values are $l_d = 0.5-1.0$ and $\beta = 0.5$. A detailed study with regard to the performance of DBIEM with the desingularization parameters was reported in (Cao *et al.* 1991). l_d is fixed at 0.85 in our work.

Once the above integral equations using isolated Rankine source are solved at each time step, the fluid velocity in Eqs. (2) and (3) can be calculated from direct derivatives

$$\mathbf{V} = \nabla \phi(p, t) = \sum_{i=1}^N \sigma(q_i, t) \nabla \left(\frac{1}{r_{pq_i}} \right) \quad (13)$$

4. Time-stepping integration scheme

In order to obtain the velocity potential and free surface elevation at each time step, the fourth-order predictor-corrector Adams-Bashforth-Moulton scheme (ABM4) and mixed Eulerian-Lagrangian (MEL) methods are used. Integrating Eqs. (2) and (3) by ABM4 and MEL is called time marching. Using the total derivative $\delta / \delta t = \partial / \partial t + \vec{v} \cdot \nabla$, the fully nonlinear free surface conditions can be modified as follows in Lagrangian frame

$$\frac{\delta \phi}{\delta t} = -g\eta - \frac{1}{2} \nabla \phi \nabla \phi + \nabla \phi \cdot \vec{v} \quad (14)$$

$$\frac{\delta \eta}{\delta t} = \frac{\partial \phi}{\partial z} - (\nabla \phi - \vec{v}) \cdot \nabla \eta \quad (15)$$

where \vec{v} represents the node velocity on the free surface. On the moving node on the free surface with semi-Lagrangian approach, $\vec{v} = (0, 0, \delta \eta / \delta t)$, the node is allowed to move only in the vertical direction. Therefore, the free surface boundary conditions can be further expressed as

$$\frac{\delta \phi}{\delta t} = -g\eta - \frac{1}{2} \nabla \phi \nabla \phi + \frac{\partial \phi}{\partial z} \left(\frac{\partial \phi}{\partial z} - \frac{\partial \phi}{\partial x} \frac{\partial \eta}{\partial x} - \frac{\partial \phi}{\partial y} \frac{\partial \eta}{\partial y} \right) \quad (16)$$

$$\frac{\delta \eta}{\delta t} = \frac{\partial \phi}{\partial z} - \frac{\partial \phi}{\partial x} \frac{\partial \eta}{\partial x} - \frac{\partial \phi}{\partial y} \frac{\partial \eta}{\partial y} \quad (17)$$

In the semi-Lagrangian approach, a time-stepping integration procedure must be employed to

obtain the values of velocity potential and wave elevation on the instantaneous free surface. After solving the boundary value problem and obtaining the fluid velocity on the free surface at each time step, the free surface boundary conditions can be treated as ordinary differential equations to be marched in time. The general form of the dynamic and kinematic boundary conditions Eqs. (16) and (17) can be rewritten as

$$\frac{\delta\phi}{\delta t} = g(\eta, \phi, t) \quad (18)$$

$$\frac{\delta\eta}{\delta t} = f(\eta, \phi, t) \quad (19)$$

ABM4 scheme Zhang *et al.* (2006) is selected for integrating Eqs. (18) and (19) with time. It is a fourth-order predictor and corrector method which requires only two evaluations of the functions $g(\eta, \phi, t)$ and $f(\eta, \phi, t)$ at each time step. In the ABM4 scheme, the velocity potential and wave elevation are firstly predicted by Adams-Bashforth method as follows

$$\phi_{t+\Delta t} = \phi_t + \frac{\Delta t}{24}(55g_t - 59g_{t-\Delta t} + 37g_{t-2\Delta t} - 9g_{t-3\Delta t}) \quad (20)$$

$$\eta_{t+\Delta t} = \eta_t + \frac{\Delta t}{24}(55f_t - 59f_{t-\Delta t} + 37f_{t-2\Delta t} - 9f_{t-3\Delta t}) \quad (21)$$

and then these are iteratively corrected by Adams-Moulton algorithm,

$$\phi_{t+\Delta t} = \phi_t + \frac{\Delta t}{24}(9g_{t+\Delta t} + 19g_t - 5g_{t-\Delta t} + g_{t-2\Delta t}) \quad (22)$$

$$\eta_{t+\Delta t} = \eta_t + \frac{\Delta t}{24}(9f_{t+\Delta t} + 19f_t - 5f_{t-\Delta t} + f_{t-2\Delta t}) \quad (23)$$

where Δt is the time interval.

5. Absorbing boundary condition

5.1 Multi-Transmitting Formula (MTF)

Liao (1996, 2002) described a general expression of one-way wave propagation and developed a system of local non-reflecting boundary conditions using space-time extrapolation. Its initial aim is to deal with the propagation of earthquake wave out of truncated surface.

In this section, the Multi-Transmitting Formula (MTF) method for treating the velocity potential ϕ in water wave field will be introduced, as shown in Fig. 2. Suppose that the point O_0 is on the truncated surface Γ_D and j are the points which are away from point O_0 along its normal vector to the fluid domain. The distance between point j and point O_0 is $jC_a\Delta t$ along the normal vector of point O_0 , where C_a , related to physical wave speed C_x , is the artificial wave speed.

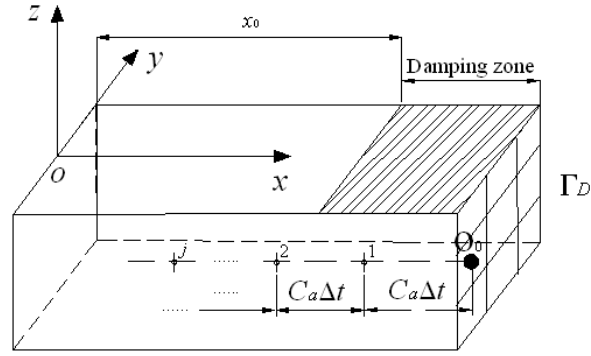


Fig. 2 Radiation condition of the numerical wave tank

According to the theory of MTF, the velocity potential on Γ_D may be written as

$$\phi_{O_0}^{p+1} = \sum_{j=1}^N (-1)^{j+1} C_j^N \phi_j^{p+1-j} \quad (24)$$

where integer p represents the time level, N is the order of the MTF method and C is the binomial coefficient.

In order to eliminate the effect of the frequencies, which are near to and including zero, a constant value γ_2 is used. Thus, the second-order MTF ($N=2$) can be written as Eq. (25), where γ_2 is an additional factor and set to 0.025 in this work

$$\phi_{O_0}^{p+1} = 2\phi_1^p / (1 + \gamma_2) - \phi_2^{p-1} / (1 + \gamma_2)^2. \quad (25)$$

For more details on the MTF method which has been applied to the earthquake wave and water wave field, these can be found in Liao (2002) and Xu and Duan (2008a), respectively.

5.2 Damping zone

The DZ method, for using near the end of computational domain as shown in Fig. 2, is commonly employed and achieved through the adding of extra terms on the free surface boundary conditions given in Eqs. (16) and (17) as follows

$$\frac{\delta\phi}{\delta t} = -g\eta - \frac{1}{2} \nabla\phi \nabla\phi + \frac{\partial\phi}{\partial z} \left(\frac{\partial\phi}{\partial z} - \frac{\partial\phi}{\partial x} \frac{\partial\eta}{\partial x} - \frac{\partial\phi}{\partial y} \frac{\partial\eta}{\partial y} \right) - \nu(x)\phi \quad (26)$$

$$\frac{\delta\eta}{\delta t} = \frac{\partial\phi}{\partial z} - \frac{\partial\phi}{\partial x} \frac{\partial\eta}{\partial x} - \frac{\partial\phi}{\partial y} \frac{\partial\eta}{\partial y} - \nu(x)\eta \quad (27)$$

where the $\nu(x)$ is the damping coefficient. The validity of DZ, however, is dependent on the ratio of the length of damping zone and the wave length. As the cost for absorbing low frequency waves is high, it is only useful for absorbing high frequency waves. It has been found in the literatures

that $v(x)$ mainly depends on the wave length λ and frequency ω corresponding to the incident wave prescribed at the upstream boundary. A quadratic function of the space variable x is typically used for incident wave

$$v(x) = \begin{cases} 0, & x \leq x_0 \\ \alpha\omega\left(\frac{x-x_0}{\lambda}\right)^2, & x > x_0 \end{cases} \quad (28)$$

where x_0 is the starting x -coordinate of the damping zone and α is the tuning factor. Contento *et al.* (2001) found that the reflection coefficient is less than 2% when the length of the DZ is set to be at least one wave length by using $\alpha=1.0$; as such, the tuning factor is set to 1.0 in our work.

6. Numerical results and discussions

The present model is applied to simulate the wave propagation for linear incident wave, second-order Stokes wave and irregular wave in a fully nonlinear NWT. In our simulation, the length of NWT (L) is 2 m, depth-length ratio $h/L=0.5$, and breadth-length ratio $B/L=0.25$. The NWT is divided in x -direction by $N_x=40$ intervals, in y -direction by $N_y=11$ intervals and in z -direction by $N_z=15$ intervals, as shown in Fig. 3.

Before investigating the MTF method for the fully nonlinear wave problem, the case with DZ as radiation condition is considered. The numerical results are shown in Fig. 4, where T is wave period. It is found that the length of DZ (L_{DZ}) is not sufficiently long to eliminate wave reflection with $L_{DZ}/\lambda=0.5$ and $L_{DZ}/\lambda=0.75$, where $\lambda=1.0$ m. The results show that at least one wave length is needed to eliminate most of the wave reflection, as also found by Contento *et al.* (2001).

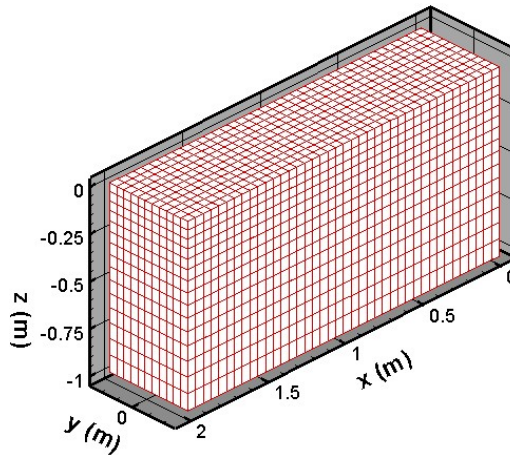


Fig. 3 Mesh for the numerical simulation of wave propagation

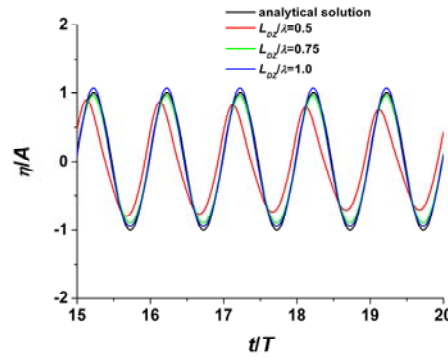


Fig. 4 Wave elevation history at ($x=0.225$ m, $y=0$) for different L_{DZ} ($\lambda=1.0$ m). Black line is linear analytical solution

Next, we consider the case with MTF+DZ as radiation condition, where L_{DZ}/λ is fixed at 0.5; here it is not sufficient to eliminate wave reflection shown in Fig. 4. From Fig. 5, it is reasonably clear that the numerical result of MTF+DZ method is better than the result of standalone DZ method. For the MTF, artificial wave speed C_a is equal to physical wave speed C_x .

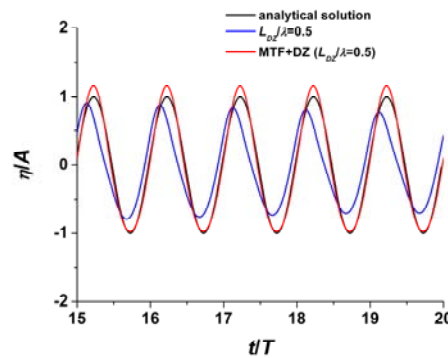


Fig. 5 Comparison of wave elevation history at ($x=0.225$ m, $y=0$) between linear analytical solution with numerical results ($\lambda=1.0$ m). Black line: linear analytical solution; Blue line: DZ as radiation condition; Red line: MTF+DZ as radiation condition

In the MTF method, we need to use an artificial wave speed C_a to find the exact position of the inner points corresponding to the control point on the truncated surface, as shown in Fig. 2. Normally, we do not need to set C_a equal to the physical wave speed C_x and yet we can still get reasonable results when C_a is in the certain prescribed range of C_x ($C_a \in 0.6 C_x \sim 1.6 C_x$) (Xu and Duan 2008a). The numerical results for different C_a are shown in Fig. 6. However, it is found that the standalone MTF method is not sufficient to transmit waves out of truncated surface when C_a is beyond the mentioned range. Thus, the MTF+DZ method is proposed as radiation condition to also

accord greater flexibility for the simulation of wave propagation in time domain. This is shown in Fig. 7(a) where $\lambda=4.0$ m and $C_a=0.6C_x$, and Fig. 7(b) where $\lambda=4.0$ m and $C_a=1.6C_x$. The effectiveness and efficiency of transmitting wave out of truncated surface has been improved obviously with the coupled MTF+DZ method.

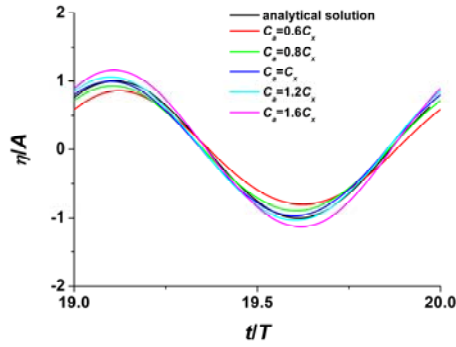


Fig. 6 Comparison of wave elevation history at ($x=0.45$ m, $y=0$) between linear analytical solution and numerical results with different artificial wave speed ($\lambda=4.0$ m)

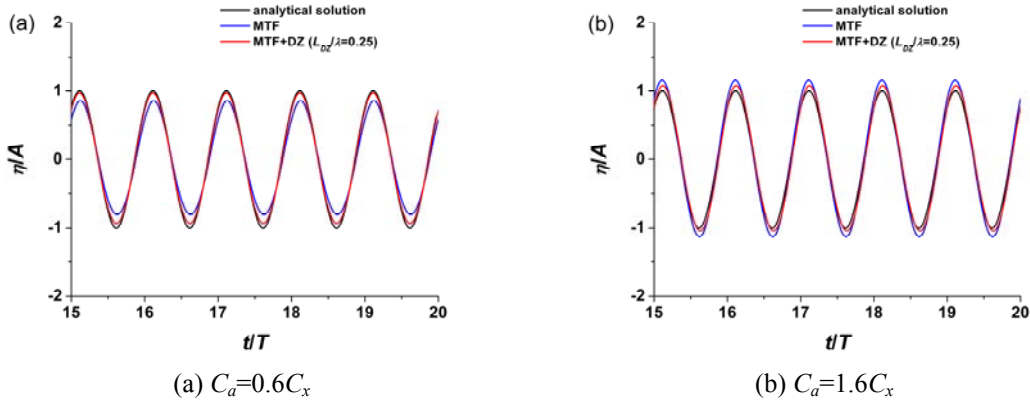


Fig. 7 Comparison of wave elevation history at ($x=0.45$ m, $y=0$) between linear analytical solution with numerical results ($\lambda=4.0$ m). Black line: linear analytical solution; Blue line: MTF as radiation condition (fully-nonlinear simulation); Red line: MTF+DZ as radiation condition (fully-nonlinear simulation)

6.1 Simulation of linear regular incident wave

The model is next applied to simulate the linear regular incident wave. We consider two cases: wave length $\lambda=1$ m and 8 m with the corresponding ratio $L_{DZ}/\lambda = 1.0$ and 0.125. For these simulations, the wave amplitude A is set to 0.02 m, Δt is taken as $T/100$ for $\lambda=1$ m and $T/200$ for

$\lambda=8$ m, L_{DZ} is set to 1.0 m and C_a is set to C_x . The numerical result is compared with linear analytical solution, as shown in Fig. 8. We can see that the numerical result obtained by the present model with coupled MTF+DZ method for the outflow radiation condition agrees fairly well with the theory after the initial transient effect. This further supports the applicability of the MTF+DZ method. It may be mentioned that a modulation function (Wang and Wu 2007), to avoid an abrupt initial condition and allow a gradual development of incident waves, is used in the numerical simulation

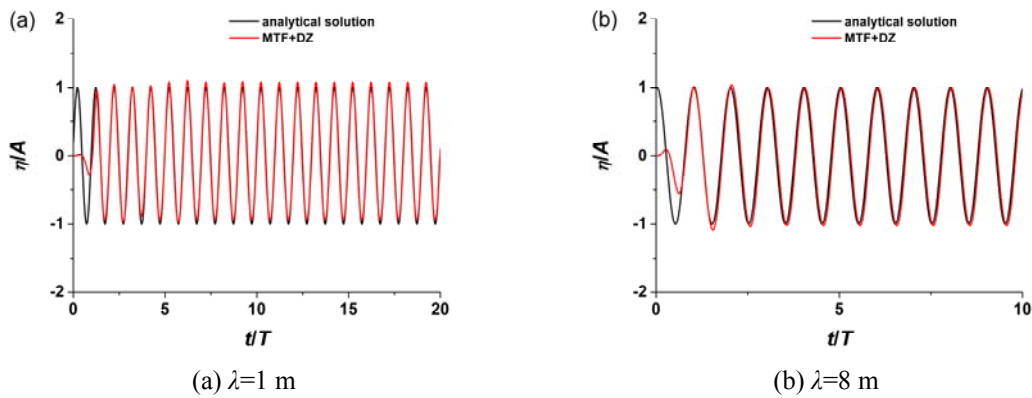


Fig. 8 Wave elevation histories at $(x=0.225$ m, $y=0)$ for different wave length. Black line: linear analytical solution; red line: MTF+DZ as radiation condition (fully-nonlinear simulation)

6.2 Simulation of second-order Stokes incident wave

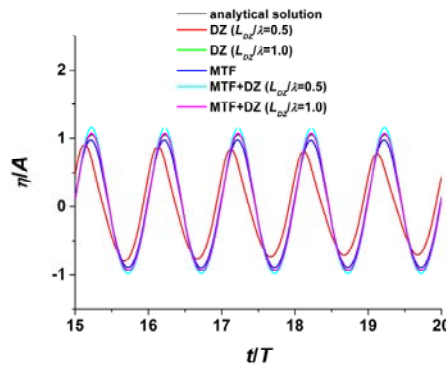


Fig. 9 Wave elevation histories at $(x=0.225$ m, $y=0)$ for $\lambda=1$ m and $A=0.02$ m. (black line: analytical solution; red line: DZ with $L_{DZ}=0.5$ m (fully-nonlinear simulation); green line: DZ with $L_{DZ}=1.0$ m (fully-nonlinear simulation); blue line: MTF (fully-nonlinear simulation); cyan line: MTF+DZ with $L_{DZ}=0.5$ m (fully-nonlinear simulation); magenta line: MTF+DZ with $L_{DZ}=1.0$ m (fully-nonlinear simulation))

The model is then applied to simulate the wave propagation of second-order Stokes waves, which have the basic characteristic of nonlinear waves of increasingly higher and sharper crest, and lower and flatter trough. The parameters for simulating the second-order Stokes waves propagation are taken as $\lambda=1$ m, $A=0.02$ m and $\Delta t=T/100$. Fig. 9 shows the wave elevation histories at $(x=0.225$ m, $y=0)$ and the numerical results are compared with second-order analytical solution. In the comparison, we can see that there are wave reflection from the truncated surface when only the DZ is used as radiation condition especially with $L_{DZ}/\lambda=0.5$. For the MTF+DZ, the results show stability and good agreement with the analytical solution. For further illustration of the wave propagation, snapshots of the free surface are shown in Fig. 10 at four different times ($t=4T$, $6T$, $8T$ and $10T$) based on MTF+DZ radiation condition.

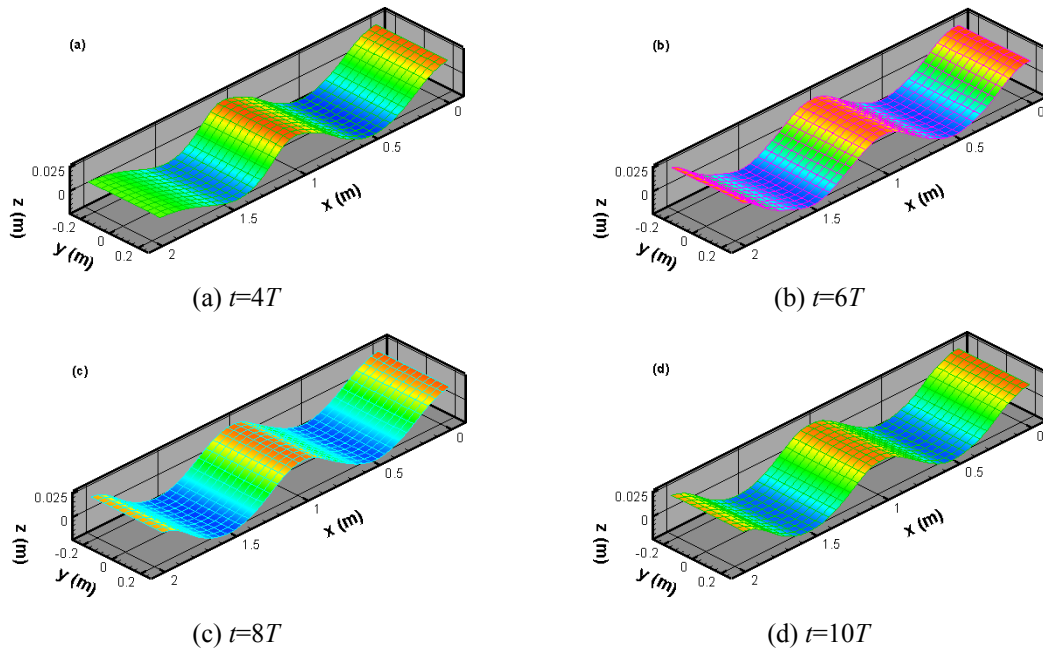


Fig. 10 Snapshots of free surface profile (fully-nonlinear simulation)

6.3 Simulation of linear irregular incident waves

Here, the linear irregular incident waves are generated using four Airy wave components with the frequencies of 5.25, 5.55, 6.73 and 7.46 rad/s (Boo 2002). The wave slope of the incident waves is fixed to be 0.035. The average frequency and wave length, used in Eq. (28), for the irregular incident waves are 6.25 rad/s and 1.67 m. The artificial wave speed C_a is set to the average wave velocity of 1.60 m/s and L_{DZ} is equal to 1m. The wave elevation history and its comparison with the corresponding linear analytical solution are shown in Fig. 11.

It is clear that the numerical result based on MTF+DZ agrees well with the analytical solution. The fully nonlinear result obtained by MTF+DZ method shows the typical features: sharper peaks and flatter troughs. It supports that the present model is effective and can be used for simulation of fully nonlinear irregular wave propagation in time domain.

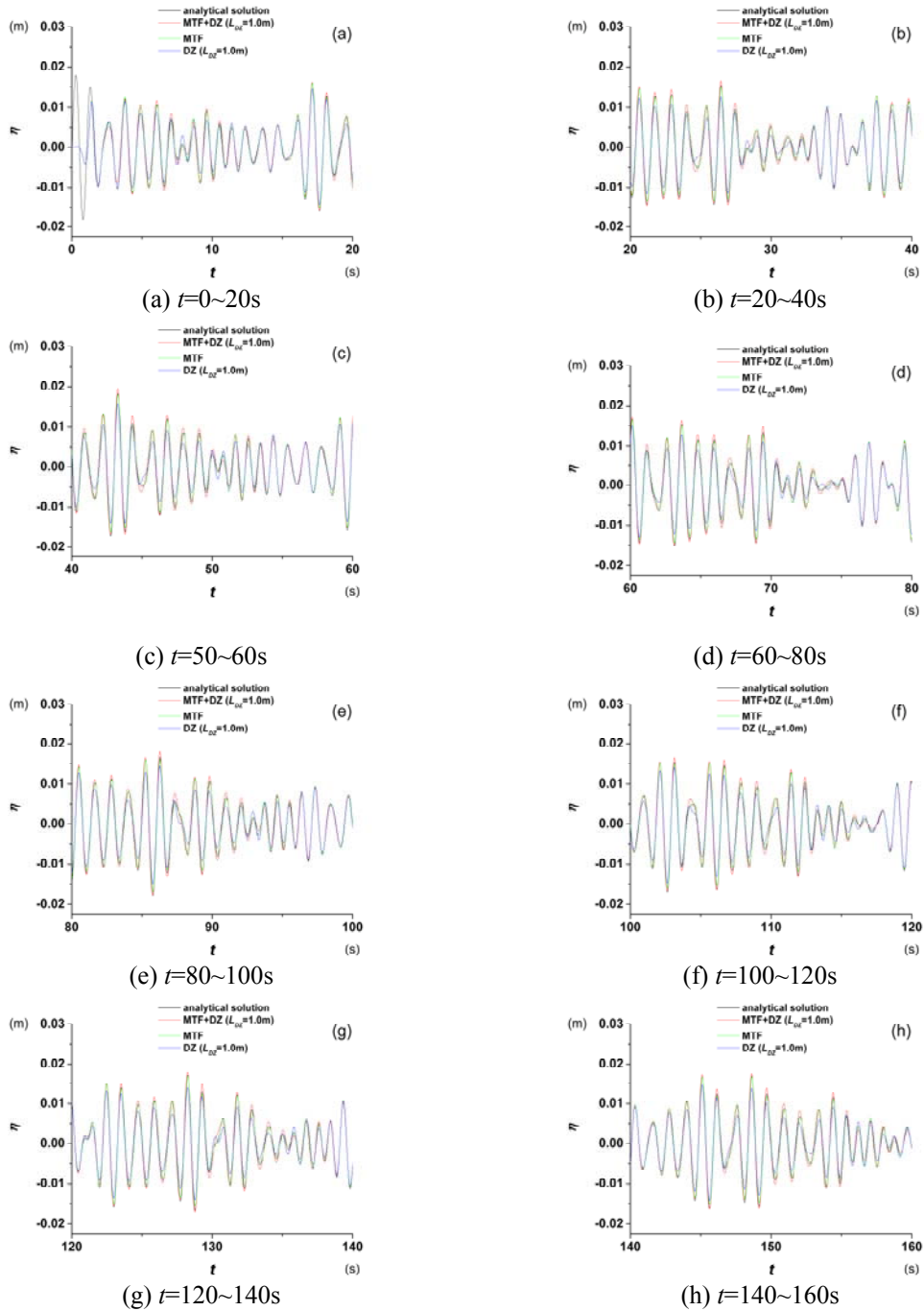


Fig. 11 Wave elevation histories at $(x=0.45\text{ m}, y=0)$. (black line: analytical solution; red line: MTF+DZ with $L_{DZ}=1.0\text{ m}$ (fully-nonlinear simulation); green line: MTF (fully-nonlinear simulation); blue line: DZ with $L_{DZ}=1.0\text{ m}$ (fully-nonlinear simulation))

7. Conclusions

In this paper, unidirectional wave propagation in a 3D NWT is solved using a DBIEM coupled with MEL time marching scheme. The position of instantaneous free surface is tracked by applying semi-Lagrangian approach. A smoothing scheme, B-spline, is applied in both longitudinal and transverse directions of the numerical wave tank to prevent saw-tooth instability. The different DZ, MTF and MTF+DZ radiation condition are employed to eliminate wave reflection on the truncated surface for 3D fully nonlinear water wave problem. It is found that the MTF+DZ method is accurate, numerically stable and can be used for the simulation of 3D fully nonlinear wave propagation due to linear incident wave, second-order incident wave and irregular incident waves.

Acknowledgements

This paper was made possible by the support of NPRP 08-691-2-289 grant from Qatar National Research Fund (QNRF). The statements made herein are solely the responsibility of the authors.

References

- Baker, G.R., Meiron, D.I. and Orszag, S.A (1981), "Applications of a generalized vortex method to nonlinear free-surface flows", *Proceedings of the 3rd International Conference on Numerical Ship Hydrodynamics*, Paris, France.
- Beck, R.F., Cao, Y. and Lee, T.H. (1993), "Fully nonlinear water wave computations using the desingularized method", *Proceedings of the 6th International Conference on Numerical Ship Hydrodynamics*, Iowa.
- Boo, S.Y. (2002), "Linear and nonlinear irregular waves and forces in a numerical wave tank", *Ocean Eng.*, **29**(5), 475-493.
- Cao, Y., Schultz, W.W. and Beck, R.F. (1991), "Three dimensional desingularized boundary integral methods for potential problems", *Int. J. Numer. Meth. Fl.*, **12**(8), 785-803.
- Celebi, M.S., Kim, M.H. and Beck, R.F. (1998), "Fully nonlinear 3-D numerical wave tank simulation", *J. Ship Res.*, **42**(1), 33-45.
- Clamond, D., Fructus, D., Grue, J. and Kristiansen, Ø. (2005), "An efficient model for three-dimensional surface wave simulations. Part II: Generation and absorption", *J. Comput. Phys.*, **205**(2), 686-705.
- Clémen, A. (1996), "Coupling of two absorbing boundary conditions for 2D time-domain simulations of free surface gravity waves", *J. Comput. Phys.*, **126**(1), 139-151.
- Cointe, R., Geyer, P., King, B., Molin, B. and Tramoni, M. (1990), "Nonlinear and linear motions of a rectangular barge in a perfect fluid", *Proceedings of the 18th Symposium on Naval Hydrodynamics*, Ann Arbor, Michigan.
- Contento, G., Codiglia, R. and D'Este, F. (2001), "Nonlinear effects in 2D transient nonbreaking waves in a closed flume", *Appl. Ocean Res.*, **23**(1), 3-13.
- Dai, Y.S. and Duan, W.Y. (2008), *Potential flow theory of ship motions in waves*, National Defence Industry Press, Beijing, China. (in Chinese)
- Duan, W.Y. and Zhang T.Y. (2009), "Non-reflecting simulation for fully-nonlinear irregular wave radiation", *Proceedings of the 24th International Workshop on Water Wave and Floating Bodies*, Russia.
- Forristall, G.Z. (1985), "Irregular wave kinematics from a kinematic boundary condition fit (KBCF)", *Appl. Ocean Res.*, **7**(4), 202-212.
- Koo, W.C. and Kim, M.H. (2007), "Fully nonlinear wave-body interactions with surface-piercing bodies",

- Ocean Eng.*, **34**(7), 1000-1012.
- Liao, Z.P. (1996), "Extrapolation non reflecting boundary conditions", *Wave Motion*, **24**, 117-138.
- Liao, Z.P. (2002), *Introduction to wave motion theories for engineering*, Science Press, Beijing, China (in Chinese).
- Newman, J.N. (2010), "Analysis of wave generators and absorbers in basins", *Appl. Ocean Res.*, **32**(1), 71-82.
- Orlanski, I. (1976), "A simple boundary condition for unbounded hyperbolic flows", *J. Comput. Phys.*, **21**(3), 251-269.
- Sclavounos, P.D. and Nakos, D.E. (1989), "Stability analysis of panel methods for free surface flows with forward speed", *Proceedings of the 17th Symposium on Naval Hydrodynamics*, Hague, Netherlands.
- Wang, C.Z. and Wu, G.X. (2007), "Time domain analysis of second-order wave diffraction by an array of vertical cylinders", *J. Fluid. Struct.*, **23**(4), 605-631.
- Xu, G. and Duan, W.Y. (2008a), "Time domain simulation for water wave radiation by floating structures (Part A)", *J. Marine Sci. Appl.*, **7**(4), 226-235.
- Xu, G. and Duan, W.Y. (2008b), "Time domain simulation of irregular wave diffraction", *Proceedings of the 8th International Conference on Hydrodynamics*, Nantes, France.
- Zhang, C.W. and Duan, W.Y. (2012), "Numerical study on a hybrid water wave radiation condition by a 3D boundary element method", *Wave Motion*, **49**(5), 525-543.
- Zhang, X.T., Khoo, B.C. and Lou, J. (2006), "Wave propagation in a fully nonlinear numerical wave tank: a desingularized method", *Ocean Eng.*, **33**(17-18), 2310-2331.
- Zhang, X.T., Khoo, B.C. and Lou, J. (2007), "Application of desingularized approach to water wave propagation over three-dimensional topography", *Ocean Eng.*, **34**(10), 1449-1458.